

Clustering signatures classify directed networks

S. E. Ahnert*

Theory of Condensed Matter, Cavendish Laboratory, JJ Thomson Avenue, Cambridge CB3 0HE, United Kingdom

T. M. A. Fink

INSERM U900, CNRS UMR144, and Curie Institute, Paris F-75248, France

and Ecole des Mines de Paris, ParisTech, Fontainebleau, F-77300 France

(Received 30 October 2007; revised manuscript received 4 June 2008; published 18 September 2008)

We use a clustering signature, based on a recently introduced generalization of the clustering coefficient to directed networks, to analyze 16 directed real-world networks of five different types: social networks, genetic transcription networks, word adjacency networks, food webs, and electric circuits. We show that these five classes of networks are cleanly separated in the space of clustering signatures due to the statistical properties of their local neighborhoods, demonstrating the usefulness of clustering signatures as a classifier of directed networks.

DOI: [10.1103/PhysRevE.78.036112](https://doi.org/10.1103/PhysRevE.78.036112)

PACS number(s): 89.75.-k, 89.65.Ef

I. INTRODUCTION

Many types of complex networks have been studied over the past decade [1], ranging from social collaboration networks [2] and the internet [3] to genetic regulatory networks [4] and transport networks [5]. This research has revealed remarkable similarities in the properties of many different types of real-world networks, such as scale-free topologies [6] and small-world connectivity [7]. However, with a few exceptions [8–11], most of the research thus far has concentrated on undirected networks, that is, networks in which the edges between nodes are not oriented. This is partially because directed networks allow a much more complicated connectivity. For example, in an undirected network there is only one way to form a triangle between three unlabeled nodes, whereas directed networks allow seven distinct triangles (see Fig. 1). The relative frequency of these seven triangles in real-world networks has been studied in the context of network motifs [12], which have been used to identify superfamilies of networks [13]. In each of these superfamilies, particular motifs occur either more or less frequently, compared to the null case, and the combination of over- and underexpressed motifs is unique to a given superfamily.

II. CLUSTERING SIGNATURE

Here we use a *clustering signature* to classify a wide range of complex directed networks. The components of this four-dimensional quantity consist of a recent generalization [11] of the undirected clustering coefficient [7] to directed networks. By normalizing it we can map this quantity to the interior of a tetrahedron, thereby providing an effective means for visualizing and comparing the local connectivity of directed networks. We find that different types of directed real-world networks cluster in distinct regions in this tetrahedron, revealing the different roles played by the nodes in these networks.

For undirected networks the *clustering coefficient* of a node i is defined [7] as

$$c_i = \frac{\sum_{j,k} a_{ij} a_{jk} a_{ik}}{d_i(d_i - 1)/2} = \frac{\sum_{j,k} a_{ij} a_{jk} a_{ik}}{\sum_{j,k} a_{ij} a_{ik}},$$

where $j < k$ and $j \neq i \neq k$, and d_i is the degree of node i . This corresponds to the number of triangles in the network which include node i , divided by the number of pairs of bonds which include i , which represent potential triangles.

In the past the task of defining a clustering coefficient in directed networks has proven difficult, as there is more than one way of forming a triangle (see Fig. 1). However, in the very recent literature [11], advances have been made in this direction, and we use a classification of triangles which is equivalent to that introduced in [11].

Consider three nodes, of which one is labeled. For these there are four distinct “basis” triangles with a single edge between each pair of nodes. Furthermore there are three types of edge pairs for these nodes which can connect the labeled node to its two unlabeled neighbors. These are the three potential triangles of directed networks. We show these four basis triangles and the three potential triangles in Fig. 2. One of the four basis triangles is the feedback (FB) loop and the remaining three are feedforward (FF) loops. The three feedforward loops differ in the in-degree of the labeled node (shown black): the labeled node has in-degree 0 for FF_A , in-degree 1 for FF_B , and in-degree 2 for FF_C . Thus one can construct four clustering coefficients for each node, one for

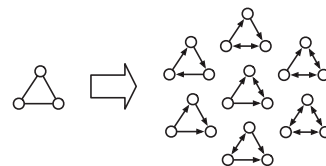


FIG. 1. Directed networks are much more complex than undirected ones. In undirected networks three unlabeled nodes can form only one sort of triangle (left), whereas in directed networks there are seven distinct triangles (right).

*sea31@cam.ac.uk

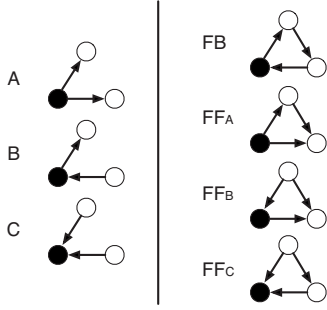


FIG. 2. The three potential triangles (left column) and four basis triangles (right column) for one labeled node (black). The basis triangles divide into a feedback (FB) loop and three feedforward (FF) loops. Note that all seven triangles shown in Fig. 1 can be recreated by superposing feedforward and feedback loops.

each type of loop [11]. Based on the clustering coefficient for undirected networks, the number of triangles N is divided by the number of potential triangles M . This gives a clustering signature for each node $\mathbf{C}^{(i)}$ given by

$$\mathbf{C}^{(i)} = \left(\frac{N_{\text{FB}}^{(i)}}{M_B^{(i)}}, \frac{N_{\text{FF}_A}^{(i)}}{M_A^{(i)}}, \frac{N_{\text{FF}_B}^{(i)}}{M_B^{(i)}}, \frac{N_{\text{FF}_C}^{(i)}}{M_C^{(i)}} \right),$$

where

$$\begin{aligned} M_A^{(i)} &= \sum_{j,k} a_{ij}a_{ik}, & M_B^{(i)} &= \sum_{j,k} a_{ij}a_{ki}, & M_C^{(i)} &= \sum_{j,k} a_{ji}a_{ki}, \\ N_{\text{FB}}^{(i)} &= \sum_{j,k} a_{ij}a_{jk}a_{ki}, & N_{\text{FF}_A}^{(i)} &= \sum_{j,k} a_{ij}a_{kj}a_{ik}, \\ N_{\text{FF}_B}^{(i)} &= \sum_{j,k} a_{ij}a_{kj}a_{ki}, & N_{\text{FF}_C}^{(i)} &= \sum_{j,k} a_{ji}a_{kj}a_{ki}, \end{aligned} \quad (1)$$

and where a_{ij} signifies a directed connection from node i to node j . The sums now run over all possible j, k such that $i \neq j \neq k \neq i$, and there is no longer a constraint of $j < k$. Note that $M_A^{(i)}$ and $M_C^{(i)}$ involve double counting, which corresponds to the two possible ways in which both FF_A and FF_C can be formed from $M_A^{(i)}$ and $M_C^{(i)}$. The set of these four quantities forms the clustering signature of a directed network.

As the clustering signature is a point in four-dimensional space, and thus is hard to visualize, we normalize the signature and omit the first dimension. In the resulting three-dimensional space each signature—represented as a point—lies inside a tetrahedron, the vertices of which are located at the origin (0,0,0) and the points (1,0,0), (0,1,0), and (0,0,1). Hence this tetrahedron is spanned by orthogonal unit vectors, which represent the three normalized feedforward loop components. The magnitude of the fourth component, representing the feedback loop, is given by the perpendicular distance between a (111) plane running through that point and the origin (with the actual component of the normalized signature being $\sqrt{3}$ times that distance). The normalized signature is defined by

$$\tilde{\mathbf{C}}^{(i)} = \frac{\mathbf{C}^{(i)}}{T^{(i)}},$$

where

$$T^{(i)} = \frac{N_{\text{FB}}^{(i)}}{M_B^{(i)}} + \frac{N_{\text{FF}_A}^{(i)}}{M_A^{(i)}} + \frac{N_{\text{FF}_B}^{(i)}}{M_B^{(i)}} + \frac{N_{\text{FF}_C}^{(i)}}{M_C^{(i)}}$$

Note that this normalization is not the standard vector normalization which divides by the modulus of the vector. It is equivalent to the normalization discussed in Eq. (18) in [11].

We can then calculate the average normalized clustering signature over all N nodes i of a given network as

$$\tilde{\mathbf{C}} = \frac{1}{N} \sum_{i=1}^N \tilde{\mathbf{C}}^{(i)}.$$

In the following we will refer to the four components of the average normalized clustering signature $\tilde{\mathbf{C}}$ as \tilde{C}_{FB} , \tilde{C}_{FF_A} , \tilde{C}_{FF_B} , and \tilde{C}_{FF_C} .

III. CLASSIFICATION OF DIRECTED NETWORKS

We calculate the clustering signatures of 16 directed real-world networks. These networks fall into five different classes: electric circuits, genetic transcription networks, social networks, language networks, and food webs. We show that these five classes are clearly separated in the space of normalized clustering signatures. To measure how tightly the groups are clustered we employ a k -means clustering algorithm which cleanly separates these networks into their respective classes, with 89% of total variance explained. These k -means centroids thus provide an effective classifier of directed networks. All k -means clustering is done in the three-dimensional space of $(\tilde{C}_{\text{FF}_A}, \tilde{C}_{\text{FF}_B}, \tilde{C}_{\text{FF}_C})$, which corresponds to the interior of the tetrahedron. The location of the 16 networks in the clustering signature tetrahedron can be seen in Fig. 3. In the following we describe the results for the different classes in detail. These results are seen in Table I.

Food webs. The three food webs studied represent a variety of ecosystems [14]: the Chesapeake Bay Mesohaline Net ($N=39$ nodes, $E=177$ edges) [15], the Everglades Graminoid Marshes ($N=69$, $E=916$) [16], and the Florida Bay Trophic Exchange Matrix ($N=128$, $E=2106$) [17]. In the clustering signature of these food webs the FF_B component is particularly prominent, with $\tilde{C}_{\text{FF}_B} > 0.42$. This translates into an increased likelihood that, if species B is eaten by species A and eats species C (a scenario corresponding to B in Fig. 2), then species A also eats species C —in a food web, this is a plausible scenario.

Transcription networks. In the two transcription networks, in the species *Escherichia coli* ($N=423$, $E=519$) and *Saccharomyces cerevisiae* ($N=688$, $E=1079$) [12], the clustering signature shows a highly dominant FF_C component ($\tilde{C}_{\text{FF}_C} > 0.62$). This signifies a markedly increased likelihood that, if gene C is regulated by genes A and B , then gene A also regulates gene B , or vice versa. Feedforward loops have been

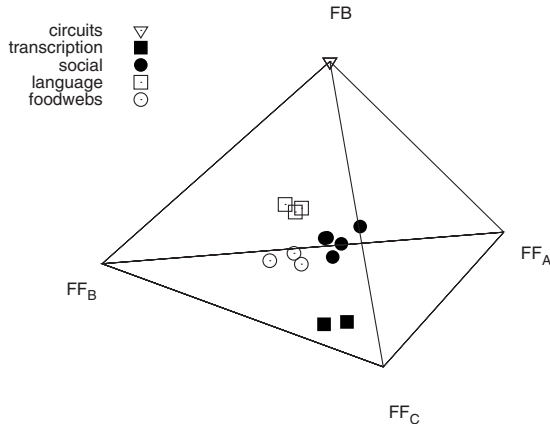


FIG. 3. Clustering signature tetrahedron with the positions of the 16 networks of five different types (see legend). k -means clustering separates these classes perfectly. The tetrahedron corresponds to the feedforward subspace of the normalized clustering signatures, i.e., $(\tilde{C}_{FF_A}, \tilde{C}_{FF_B}, \tilde{C}_{FF_C})$, so that the FB vertex corresponds to $(0,0,0)$, and the FF_A , FF_B , and FF_C vertices correspond to the $(1,0,0)$, $(0,1,0)$, and $(0,0,1)$ points, respectively. If a network has only feedback loops and no feedforward loops (such as the electric circuits studied in this paper), it will be located at the base of the tetrahedron. Conversely, a network without any feedback loops will be located at the top of the tetrahedron. The location of a network relative to the FF_A , FF_B , and FF_C vertices signifies the relative dominance of the given node roles (see Fig. 2). As an illustration, consider the transcription networks (black squares) which have a k -means centroid of $(0.145, 0.232, 0.622)$. The normalization implies that $\tilde{C}_{FB} = 1 - 0.145 - 0.232 - 0.622 = 0.001$ so that these networks will be located at the base of the tetrahedron. The FF_A component is also negligible, so that the networks lie on the edge opposite the FF_A vertex, and closer to FF_C than FF_B because the FF_C component is larger.

shown to occur frequently in transcription networks [18]. The reason that the FF_A component of the clustering signature is suppressed is because many genes that are located at the top of a feedforward hierarchy (i.e., in the FF_A position) regulate many other genes, which increases M_A and dilutes the FF_A component. If a gene is regulated by two other genes, however, as represented by the FF_C scenario, the probability that all three form a feedforward loop is large, since the in-degrees in these transcription networks are small.

Language networks. These three word-adjacency networks for English ($N=7724$, $E=46281$), French ($N=9424$, $E=24295$), and Japanese ($N=3177$, $E=8300$) [13] show increased FB (with $\tilde{C}_{FB} > 0.32$) and FF_B (with $\tilde{C}_{FF_B} > 0.31$) components. This reflects the fact that words fall into several categories such as nouns, adjectives, verbs, and conjunctions, and that words of the same category are rarely adjacent. This is why the FF_A and FF_C components are suppressed, as it requires words B and C , which can both follow (or precede) word A , to be able to appear adjacent to each other as well. Furthermore, the FF_B component is also enhanced by the presence of inserted words, such as adjectives, since it represents words that could be omitted without making the grammar invalid.

Social networks. The five social networks represent a

TABLE I. Comparison of the clustering signature properties of 16 networks of five types. The food webs, transcription networks, language networks, and social networks are distinguished using k -means clustering with 89% of variance explained. Electric circuits were not included in the k -means clustering as they form an infinitely tight cluster. The k -means centroids in the space of normalized, clustering signatures are given in the table. Due to the normalization, the fourth component of the normalized signature is implicitly given by the other three: $\tilde{C}_{FB} = 1 - \tilde{C}_{FF_A} - \tilde{C}_{FF_B} - \tilde{C}_{FF_C}$. Note that the neutral point, corresponding to undirected networks, lies at $(0.25, 0.25, 0.25, 0.25)$.

networks	k-means centroid $(\tilde{C}_{FF_A}, \tilde{C}_{FF_B}, \tilde{C}_{FF_C})$	dominant component(s)
Food webs (3)	0.283, 0.445, 0.195	 > 0.42
Transcription (2)	0.145, 0.232, 0.622	 > 0.62
Language (3)	0.160, 0.321, 0.178	 > 0.32 > 0.31
Social (5)	0.372, 0.295, 0.183	 > 0.30
Circuits (3)	—	 = 1.0

wide range of social interactions, from hyperlinks between political web logs ($N=1491$, $E=19090$) [19], relationships between prison inmates ($N=67$, $E=182$) [20], selection of team partners ($N=32$, $E=96$) [21], and interactions in an African tailor shop at two different times ($N=39$, $E=109$; $N=39$, $E=147$) [22]. Many social networks are undirected, and the fact that the five directed social networks studied here are close to the neutral normalized clustering signature $\tilde{C}_N = (0.25, 0.25, 0.25, 0.25)$ is an indicator that even directed social networks are rather symmetric. To quantify this one can consider a measure of reciprocity introduced in the re-

cent literature [23], which takes values between 1 and -1 indicating whether reciprocal links occur more or less often than expected by chance. The five social networks studied here have values of reciprocity between 0.11 and 0.49, which indicates a definite but not overwhelming presence of reciprocal links. The observation that social networks are approximately symmetric is not surprising as social interactions are typically reciprocal, and when they are not, the direction of a social interaction is often difficult to define. Therefore the direction of the edges in a directed social network has to be defined particularly carefully, as reversing the direction of all edges will swap the \tilde{C}_{FF_A} and \tilde{C}_{FF_C} components. In the five social networks studied here, the direction of the edge can be understood as an imbalance of benefits between the two social agents. In the tailor shop this measures whether person B is more useful to person A than A to B . If so, the arrow points from A to B . In political web logs, the owner of a site A chooses to link to another site B , representing a use of site B . In this case the edge would also go from A to B . In the prison, where inmate A expresses positive sentiments toward prisoner B , the arrow too goes from A to B . Students choosing other students as co-workers on a team are an equivalent case. Overall, the deviation of the social networks from the neutral point \tilde{C}_N is small, and is most marked in the FF_A component (with $\tilde{C}_{FF_A} > 0.30$). To understand this, consider a person A who names two others B and C as friends. If B or C is also popular, chances are that the less popular one of the two will choose the more popular one as their friend as well. This creates a feedforward loop with node A as the labeled node of a FF_A loop (see Fig. 2). The suppressed FF_C component, on the other hand, may represent popular individuals who are chosen by many, who in turn would not choose each other.

Electric circuits. Due to their specific design, these three circuits ($N=122$, $E=189$; $N=252$, $E=399$; $N=512$, $E=819$) from [12], which represent digital fractional multipliers, contain only feedback loops, placing them at the FB vertex of the clustering signature tetrahedron.

IV. DISCUSSION

To demonstrate that the clustering signature depends only on the local connectivity of directed network edges and not on differences in the overall density of edges in the networks, we flip the direction of edges between all connected pairs of nodes, with probability one-half. This keeps the undirected connectivity (and thus the edge density) constant, while destroying the distinction between the four loops FB, FF_A , FF_B , and FF_C . If clustering signatures are dependent only on the local connectivity of directed edges, then destroying the information about the direction of edges should move all randomized real-world networks to the center of the tetrahedron.

This prediction is indeed confirmed by the results for ten such randomizations on each of the 16 networks. After randomization, all networks lie very close to the neutral point of $\tilde{C}_N=(0.25,0.25,0.25,0.25)$ with averages always between 0.22 and 0.27, and in most cases between 0.24 and 0.26. The neutral point lies within one standard deviation in all cases. This confirms that the clustering signature tetrahedron is an effective way of measuring the differences in the local connectivity of directed networks.

Note that, for the networks examined, the number of nodes and edges varies widely—both within the five groups of networks and between them. The fact that the types of networks are nevertheless clearly separated, together with the randomization test discussed above, suggests that the classification according to clustering signatures is independent of the network size. Only for very sparse, small graphs would one expect the size of the network to matter in the form of a visible discretization of clustering signature values, which may coarsen the classification. While the dimensional limitations mean that additional network features cannot easily be included in three dimensions, one could achieve such a combined analysis by constructing a larger feature vector—containing the clustering signature—which could then be analyzed using multivariate methods such as principal component analysis or canonical variable analysis [24].

Finally, clustering signatures can be generalized to weighted directed networks in a straightforward way by using the ensemble approach [25]. This requires a choice of mapping from weights w_{ij} to the unit interval: $w_{ij} \in \mathbb{R} \rightarrow p_{ij} \in [0, 1]$, which depends on the nature of the weights. These p_{ij} replace the adjacency matrix entries a_{ij} in all seven expressions for M and N in Eq. (1), in analogy to the ensemble clustering coefficient for undirected networks discussed in [25]. Note that, in the case of this weighted generalization, the individual clustering coefficients differ from those defined for the weighted case in [11].

In conclusion, our analysis reveals that different types of directed real-world networks are characterized by their clustering signature. The relative strength of the four components of the signature is an indicator of the way in which nodes connect to their neighborhood. Thus clustering signatures offer an effective method for the classification of directed networks. They also provide an intuitive three-dimensional space in which the local connectivity of directed networks can be visualized and compared.

ACKNOWLEDGMENTS

S.E.A. was supported by The Leverhulme Trust, U.K. This work was funded in part by the Defense Advanced Research Projects Agency (DARPA) Fundamental Laws of Biology (FunBio) Grant No. HR 0011-05-1-0057.

- [1] R. Albert and A.-L. Barabasi, *Rev. Mod. Phys.* **74**, 47 (2002).
- [2] M. E. J. Newman, *Proc. Natl. Acad. Sci. U.S.A.* **98**, 404 (2001).
- [3] M. Faloutsos, P. Faloutsos, and C. Faloutsos, in *Proceedings of the ACM SIGCOMM*, edited by R. Guerin [Comput. Commun. Rev.29, 251 (1999)].
- [4] S. Maslov and K. Sneppen, *Science* **296**, 910 (2002).
- [5] A. Barrat, M. Barthelemy, R. Pastor-Satorras, and A. Vespignani, *Proc. Natl. Acad. Sci. U.S.A.* **101**, 3747 (2004).
- [6] A.-L. Barabasi and R. Albert, *Science* **286**, 509 (1999).
- [7] D. J. Watts and S. H. Strogatz, *Nature (London)* **393**, 440 (1998).
- [8] L. F. Costa, *Phys. Rev. Lett.* **93**, 098702 (2004).
- [9] A. Capocci, V. D. P. Servedio, F. Colaiori, L. S. Buriol, D. Donato, S. Leonardi, and G. Caldarelli, *Phys. Rev. E* **74**, 036116 (2006).
- [10] G. Fagiolo, *Aust. J. Constr. Econ. Build.* **3**, 1 (2007).
- [11] G. Fagiolo, *Phys. Rev. E* **76**, 026107 (2007).
- [12] R. Milo, S. Shen-Orr, S. Itzkovitz, N. Kashtan, D. Chklovskii, and U. Alon, *Science* **298**, 824 (2002).
- [13] R. Milo, S. Itzkovitz, N. Kashtan, R. Levitt, S. Shen-Orr, I. Ayzenshtat, M. Sheffer, and U. Alon, *Science* **303**, 1538 (2004).
- [14] The food web data can be downloaded from <http://vlado.fmf.uni-lj.si/pub/networks/data/bio/foodweb/foodweb.htm>.
- [15] D. Baird and R. E. Ulanowicz, *Ecol. Monogr.* **59**, 329 (1989).
- [16] R. E. Ulanowicz, J. J. Heymans, and M. S. Egnotovich, Chesapeake Biological Laboratory, Solomons, MD 20688-0038, USA, Ref. No. [UMCES] CBL 00-0176, 2000 (unpublished).
- [17] R. E. Ulanowicz, C. Bondavalli, and M. S. Egnotovich, Chesapeake Biological Laboratory, Solomons, MD 20688-0038, USA, Ref. No. [UMCES]CBL 98-123, 1998 (unpublished).
- [18] S. Mangan and U. Alon, *Proc. Natl. Acad. Sci. U.S.A.* **100**, 11980 (2003).
- [19] L. A. Adamic and N. Glance, Proceedings of the WWW-2005 Workshop on the Weblogging Ecosystem, 2005 (unpublished).
- [20] J. MacRae, *Sociometry* **23**, 360 (1960).
- [21] L. D. Zeleny, *Sociometry* **13**, 314 (1950).
- [22] B. Kapferer, *Strategy and Transaction in an African Factory* (Manchester University Press, Manchester, 1972).
- [23] D. Garlaschelli and M. I. Loffredo, *Phys. Rev. Lett.* **93**, 268701 (2004).
- [24] L. da F. Costa, F. A. Rodriguez, G. Travieso, and P. R. Villas Boas, *Adv. Phys.* **56**, 167 (2007).
- [25] S. E. Ahnert, D. Garlaschelli, T. M. A. Fink, and G. Caldarelli, *Phys. Rev. E* **76**, 016101 (2007).